ACS Catalysis

pubs.acs.org/acscatalysis Research Article

Selective Heterogeneous Transfer Hydrogenation from Tertiary Amines to Alkynes

Gabriel J. Roeder,[#] H. Ray Kelly,[#] Guoju Yang, Thomas J. Bauer, Gary L. Haller, Victor S. Batista, and Eszter Baráth*

Cite This: *ACS Catal.* 2021, 11, 5405−5415 Read Online

ACCESS | Metrics & More | Article Recommendations | Supporting Information

ABSTRACT: Hydrogen transfer reactions from tertiary amines to phenyl- and alkyl-substituted alkynes catalyzed by Pt and Pd supported on carbon are investigated. Evidence of a sequential two-cycle mechanism shows initial formation of the *cis* alkene as the main product. Over-reduction to form the substituted alkane can be suppressed by suitable selection of the catalyst and amine partner. The prereduced catalysts Pd/C and Pt/C show high activity with partial to complete conversion detected at 140 °C in *p*-xylene under inert conditions. Both 1-ethylpyrrolidine (1-EPyr) and *N*,*N*-diisopropylethylamine ($(^{i}Pr)_2NEt$) are active, with Pt/C− and Pd/C−$(^{i}Pr)_2NEt$ outperforming Pt/C− and Pd/C−1-EPyr for all substrates. Density functional theory calculations support the sequential nature of the two-cycle transfer hydrogenation mechanism, which results from the stronger binding of alkynes to the noble metal surfaces when compared to alkenes. Key factors critical for *cis* selectivity include formation of a metal hydride−alkylamine alkyne intermediate and sufficient surface coverage by the tertiary amine. Taken together, the reported experimental and theoretical findings show that tertiary amines play a critical role as both H donors and electronic stabilizers for *cis*-selective heterogeneous transfer hydrogenation reactions of alkynes catalyzed by noble metals supported on carbon. The activation parameters of the reaction, including activation energy (E_a) as well as enthalpy and entropy of activation ($\Delta H^{\circ\ddagger}$ and $\Delta S^{\circ\ddagger}$), exhibit a clear compensation phenomenon that provides the isokinetic temperatures for which the highest rate constant is obtained and suggest that the hydrogenation mechanism is the same for all substrates.

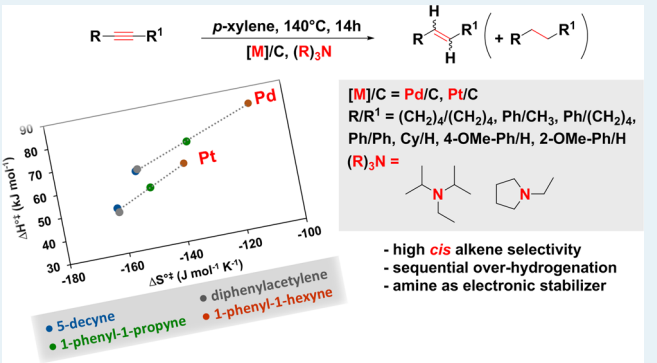

KEYWORDS: *hydrogen transfer, alkyne, noble metal, carbon support, alkyl amine, cis−trans isomer*

1. INTRODUCTION

Hydrogen transfer reactions have a multitude of uses, with applications in various synthetic and functionalization pathways of alkenes, alkynes, imines, and carbonyl compounds.[1] Such pathways involve the reduction of unsaturated compounds and can display stereoselective and enantioselective reactivity.[2] Here, we focus on the mechanism of transfer hydrogenation (TH) of phenyl- and alkyl-substituted alkynes catalyzed by noble metals (Pt and Pd) supported on carbon using tertiary alkyl amines as the H source.

Transfer hydrogenation involves intermolecular hydrogen transfer from a donor to an acceptor molecule. TH reactions are thus essentially disproportionation reactions, entailing the movement of a hydride and a proton or two protons and two electrons.[1,3] Two main mechanisms can be distinguished, including direct hydride transfer from the donor to the acceptor and indirect transfer that requires formation of a metal hydride intermediate to facilitate the hydride transfer.[1c] Transfer hydrogenation reactions allow for simplified experimental setups and reduced safety hazards compared to classic hydrogenation with H_2 gas and use common, inexpensive hydrogen sources.

Transfer hydrogenation reactions have been extensively studied, with alcohols serving as the most successful and commonly used hydrogen source in the presence of heterogeneous catalysts.[1c] Systems using 2-propanol (IPA) as the hydrogen donor also benefit from the alcohol acting as a solvent. Ammonium formate, ethanolamine, and $NaBH_4$ have been used successfully as transfer hydrogenation reagents for semihydrogenation of alkynes, representing the strategy of using alternative hydrogen sources with noble metals.[1d,f] Amines, imines, and carbonyl compounds have also been used as reducing agents.[1c] Amines have gained importance because of their capability to donate hydrogen and to form

Received: November 26, 2020
Revised: April 6, 2021

https://doi.org/10.1021/acscatal.0c05186
ACS Catal. 2021, 11, 5405−5415

surface hydrides.[1c,4] Tertiary amines form enamines[4] easily under mild reaction conditions,[4d,e] which proves their capability to serve as hydrogen sources with no or negligible side product formation[4b,e] in contrast with secondary amines.[4b,f] In fact, internal alkenes have been selectively reduced to alkanes using tertiary alkyl amines as reducing agents in combination with supported noble metal catalysts (Pd/C, Pt/C, and Rh/C) under inert conditions in a *p*-xylene solvent at 140 °C.[4a] However, the underlying reaction mechanism has not been established, and it is addressed in this paper.

The heterogeneously catalyzed selective synthesis of alkenes from alkynes[5a] always has the great advantage of chemical and thermal stability and easier product separation in comparison to homogeneous counterparts.[1c,5] Based on the success of TH with alkenes,[4a] we extend the range of substrates to include substituted alkynes that could be converted to alkenes with high stereoselectivity (and sequentially to the corresponding alkanes).

Alkyne hydrogenation is important in industrial processes including the removal of acetylene during the production of ethylene and the hydrogenation of phenylacetylene to produce a pure styrene feedstock for polymerization.[5b,c] It also serves as a key step in the synthesis of a wide variety of organic compounds.[5d] Amines have previously been used as modifiers to enhance selectivity and activity in the classic hydrogenation of alkynes with molecular hydrogen.[5e] Here, amines serve this role while also acting as the hydrogen source in the TH of alkynes.

The Lindlar catalyst (5 wt % $PdCaCO_3/Pb(OCOCH_3)_2$/quinoline)[6] is the most common industrially used heterogeneous catalyst for selective, direct hydrogenation of alkynes to the corresponding *cis* alkenes with molecular H_2. Palladium catalyzes formation of alkenes from alkynes, while $Pb(OCOCH_3)_2$ plays a positive poisoning role, suppressing over-hydrogenation by hindering hydride formation and alkene adsorption.[6] The quinoline prevents oligomerization by isolating the adsorption sites.[6] The Lindlar catalyst has been studied extensively and used successfully.[6] However, there is great interest in the development of an alternative catalyst that could avoid the need of using the highly toxic $Pb(OCOCH_3)_2$ and pressurized H_2.

Therefore, we seek TH catalysts that avoid poisoning materials and special synthesis methods such as functionalized nanoparticles[5a] while still keeping conversion, yield, and selectivity at acceptable levels. Additionally, the relative simplicity of our system facilitates a mechanistic study at the molecular level.

In the current study, we investigate tertiary amines as reducing agents in the TH reaction of alkyl/alkyl-, alkyl/phenyl-, and phenyl/phenyl-substituted alkynes on Pd/C and Pt/C. We analyze the reaction rates, turnover frequency (TOF) values, and activation parameters of the reaction on the two metals, including E_a (activation energy), $\Delta H^{\circ\ddagger}$ (enthalpy of activation), and $\Delta S^{\circ\ddagger}$ (entropy of activation). We focus on four main model substrates to elucidate the molecular origin of selectivity leading to the observed *cis* isomer dominance. Our DFT calculations show the presence of a metal hydride−alkylamine alkyne intermediate and reveal the crucial role of the amine in determining selectivity by modulating the energetics of this intermediate. The experimental results and theoretical calculations are in excellent agreement, identifying the beneficial effect of the amine acting as an electronic stabilizer of the *cis* isomer. The combined experimental and computational results show evidence of a two-cycle transfer hydrogenation mechanism (with the first cycle producing alkenes and the second producing alkanes), which is favored by the stronger binding of alkynes relative to alkenes on noble metal catalytic surfaces.

2. RESULTS AND DISCUSSION

We focus on alkynes as starting materials (Figure 1), including 5-decyne (**1**), 1-phenyl-1-propyne (**2**), 1-phenyl-1-hexyne (**3**),

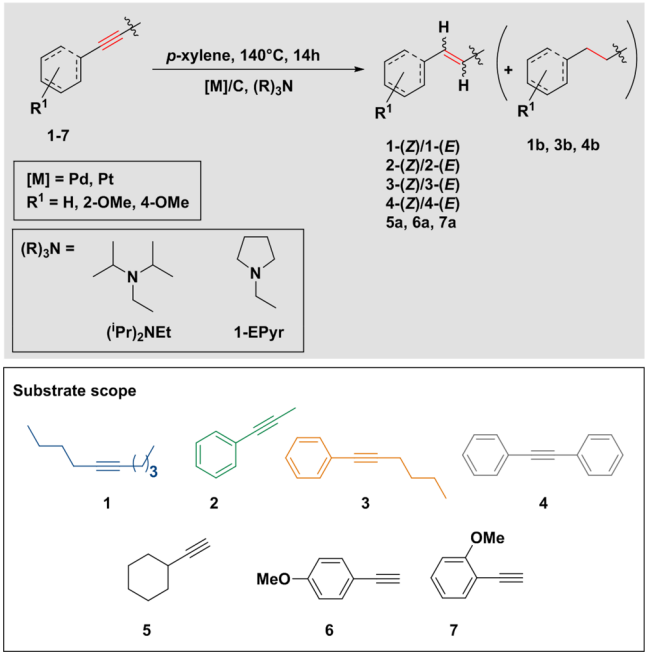

Figure 1. Reaction scheme and substrate scope of hydrogen transfer reactions with alkynes in the presence of tertiary alkyl amines as H donors.

diphenylacetylene (**4**), hexylacetylene (**5**), and 4- and 2-ethynylanisoles (**6** and **7**). These substrates were selected to analyze the effect of the steric bulkiness of the substituents on the adsorption properties and activation parameters of the reaction.

We selected Pd and Pt (10 wt %) as noble metal catalysts supported on activated carbon (commercial catalysts). The metal catalysts were activated by reduction prior to their use (see the Supporting Information for detailed activation procedure) and characterized after activation in terms of their metal loading, metal dispersion, metal particle diameter, BET surface area, and pore volume (Table 1). The metal particle size distribution was in the range of 3.5−7.1 nm based on H_2 chemisorption and TEM measurements, with a dispersion of 16.3−28.9% (for TEM analysis and XRD pattern, see the Supporting Information, Figure S1). The highest BET surface area (total) was detected for Pt/C (1532 $m^2\ g^{-1}$), while the lowest area was identified for Pd/C (1012 $m^2\ g^{-1}$).

We study the catalytic activity of all combinations of Pd/C and Pt/C with the previously demonstrated H donors such as 1-ethylpyrrolidine (1-EPyr) and *N*,*N*-diisopropylethylamine ($(^iPr)_2NEt$) (Table 2).[4a] Two interesting phenomena are extracted from our results. First, the alkene formation is stereospecific for all of the choices of a catalytic system and substrate, with the thermodynamically less favored *cis* isomer

https://doi.org/10.1021/acscatal.0c05186
ACS Catal. 2021, 11, 5405−5415

Table 1. Characterization of Noble Metals on Carbon

characterization type	catalyst Pd/C	Pt/C
metal loading (wt %)[a]	10.0	10.1
metal dispersion (%)[b]	16.3	28.9
metal particle diameter (nm)[b]	6.8	3.5
metal particle diameter (nm)[c]	7.1	3.8
BET surface area/total ($m^2\ g^{-1}$)	1012	1532
BET surface area/mesopore ($m^2\ g^{-1}$)	319	540
BET surface area/micropore ($m^2\ g^{-1}$)	693	991
pore volume/total ($cm^3\ g^{-1}$)	0.67	1.24
pore volume/mesopore ($cm^3\ g^{-1}$)	0.36	0.71
pore volume/micropore ($cm^3\ g^{-1}$)	0.31	0.53

[a]The metal content was determined with AAS. [b]Determined by H_2 chemisorption. [c]The particle size was measured by TEM (Figure S1, see the Supporting Information).

Table 2. Hydrogen Transfer with Alkynes, Catalytic Activity[a,b]

	catalyst			
	Pd/C		Pt/C	
	amine			
	$(^iPr)_2NEt$	1-EPyr	$(^iPr)_2NEt$	1-EPyr
	conversion (%), (yield (*Z*)/(*E*) (%)), [selectivity (*Z*)/(*E*) (%)]			
substrate	entry 1A	entry 1B	entry 2A	entry 2B
1	55	53	100[c]	48
	(50/5)	(48/5)	(76/17)	(43/5)
	[90/10]	[90/10]	[82/18]	[90/10]
2	30	22	90	34
	(27/3)	(20/2)	(73/17)	(31/3)
	[90/10]	[90/10]	[80/20]	[90/10]
3	41	27	100[c]	38
	(39/2)	(26/1)	(69/17)	(33/5)
	[95/5]	[96/4]	[80/20]	[87/13]
4	40	33	100[c,d]	41
	(36/4)	(30/3)	(82/18)	(38/3)
	[90/10]	[90/10]	[82/18]	[93/7]
5[e]	54	32	78	39
6[e]	16	13	24	20
7[e]	21	18	25	19

[a]Reaction conditions: substrates/entries 1 and 2 (1.0 mmol), alkyl amines (4.4 mmol), catalysts Pd/C (10 wt %, 0.1 mmol Pd) or Pt/C (10 wt %, 0.1 mmol Pt), *p*-xylene (1.5 mL), 140 °C, 14 h, under Ar and atmospheric pressure. [b]Product distribution was determined by GC(-MS) analysis with internal standards and reference materials (for the detailed procedures see the Supporting Information). [c]Over-hydrogenated, C−C single-bonded final compounds were detected (at the highest conversion level of alkynes to alkenes, the *cis*/*trans* ratio was ∼4/1). [d]The intermediately forming *trans*-stilbene remained unchanged during the over-hydrogenation reaction, and *cis*-stilbene was completely converted to 1,2-diphenyletane. [e]Terminal alkenes (**5a**, **6a**, and **7a**) were formed exclusively.

dominating the product yield (highest yield, 82% for *cis*-stilbene, Table 2, entry 2A, substrate **4**).

We observe that the Pt/C−$(^iPr)_2$NEt catalyst (Table 2, entry 2A, substrates **1**, **3**, and **4**) forms the corresponding alkane by over-hydrogenation. Importantly, the over-hydrogenation proceeds sequentially, after alkene formation, not as a parallel reaction. Therefore, it can be suppressed or enhanced to achieve selective alkene or alkane formation (Figure 2A1-A2, B1-B2, C1-C2, D1-D2, substrates **1**−**4**) with suitable conditions, such as modifying the choice of the tertiary amine. Interestingly, for substrate **4**, the intermediate *trans* isomer (4-(*E*)) is not converted any further and thus remains unchanged in the reaction mixture, while the *cis* isomer converts completely (Table 2, entry 2A; Figure 2D2). Under the same reaction conditions, using *trans*-stilbene (4-(*E*)) as a starting material shows a maximal conversion of 4% to 1,2-diphenylethane using Pt/C−$(^iPr)_2$NEt, indicating the strong inertness of the thermodynamically more stable isomer. Substrates **5**, **6**, and **7** form the corresponding terminal alkenes (**5a**, **6a**, and **7a**) as shown in Table 2 without formation of the over-hydrogenated species.

Pd/C−$(^iPr)_2$NEt and Pt/C−$(^iPr)_2$NEt are clearly the most active catalyst systems, regardless of the substrate; Pt/C exhibits the highest overall conversions for substrates **1**−**7** (Table 2). At the expense of this high activity for substrates **1**−**4** (Table 2, entry 2A), the isomer ratio of the *cis*/*trans* geometric forms is decreased to ∼4/1, and the reaction ultimately results in complete conversion to over-hydrogenated C−C single-bonded products (**1b**, **3b**, and **4b**) for substrates 1, 3 and 4 (Table 2, entry 2A). In the case of substrate **2**, only the geometric alkene isomers (**2**-(*Z*)/**2**-(*E*)) are formed with the ratio of ∼4/1 (Table 2, entry 2A).

Model compounds with alkyl/alkyl (**1**), phenyl/methyl (**2**), phenyl/hexyl (**3**), and phenyl/phenyl (**4**) substituents were investigated in detail to understand the relatively high selectivity for the *cis* isomer and the correlation between the activation parameters of the reaction and effect of the steric demand of the substrates.

To better understand the selectivity pattern produced by the catalytic systems, we analyzed the relative adsorption of the starting alkynes and intermediately forming alkenes to the metal surface as well as the hydrogenation capabilities of the metals. Importantly, the structure of the substrate influences the hydrogenation selectivity. Due to steric hindrance and accessibility, the hydrogenation of terminal olefins (saturation with molecular hydrogen) is observed to be much faster than that of internal olefins.[5a,7a] High alkene selectivity can therefore be obtained for semihydrogenation of internal alkynes due to their slower over-reduction rate.[5a,7b] Moreover, since alkene hydrogenation rates are typically faster than those of alkyne hydrogenation,[5a] the final selectivity can be credited to the stronger adsorption of the alkyne compared with that of the alkene (thermodynamic selectivity).[5a]

For semihydrogenation reactions with heterogeneous catalysts, Pd is usually preferred over Pt.[5a] Pd and Pt both have the abilities to activate and adsorb considerable amounts of molecular hydrogen. Pt is a good hydrogenation catalyst, but it does not produce stable binary hydrides, while Pd is able to form them.[7c,d] Palladium has therefore been identified as the most efficient metal in terms of activity and selectivity, which has been attributed to the stronger adsorption of the C≡C group (relative to C=C) on the Pd surface, thus preventing the over-reduction of the alkene intermediate.[5a,7e] Consistent with previous reports on hydrogenation of alkynes,[6] we did not detect any over-hydrogenated product for hydrogen transfer reactions using Pd/C with tertiary alkyl amines irrespective of the reducing agent and substrate structure (Table 2).

Reaction rates and TOF values were compared for substrates **1**−**4** (Figure 2A1−D1, A2−D2 and Table 3). The fastest initial

https://doi.org/10.1021/acscatal.0c05186
ACS Catal. 2021, 11, 5405−5415

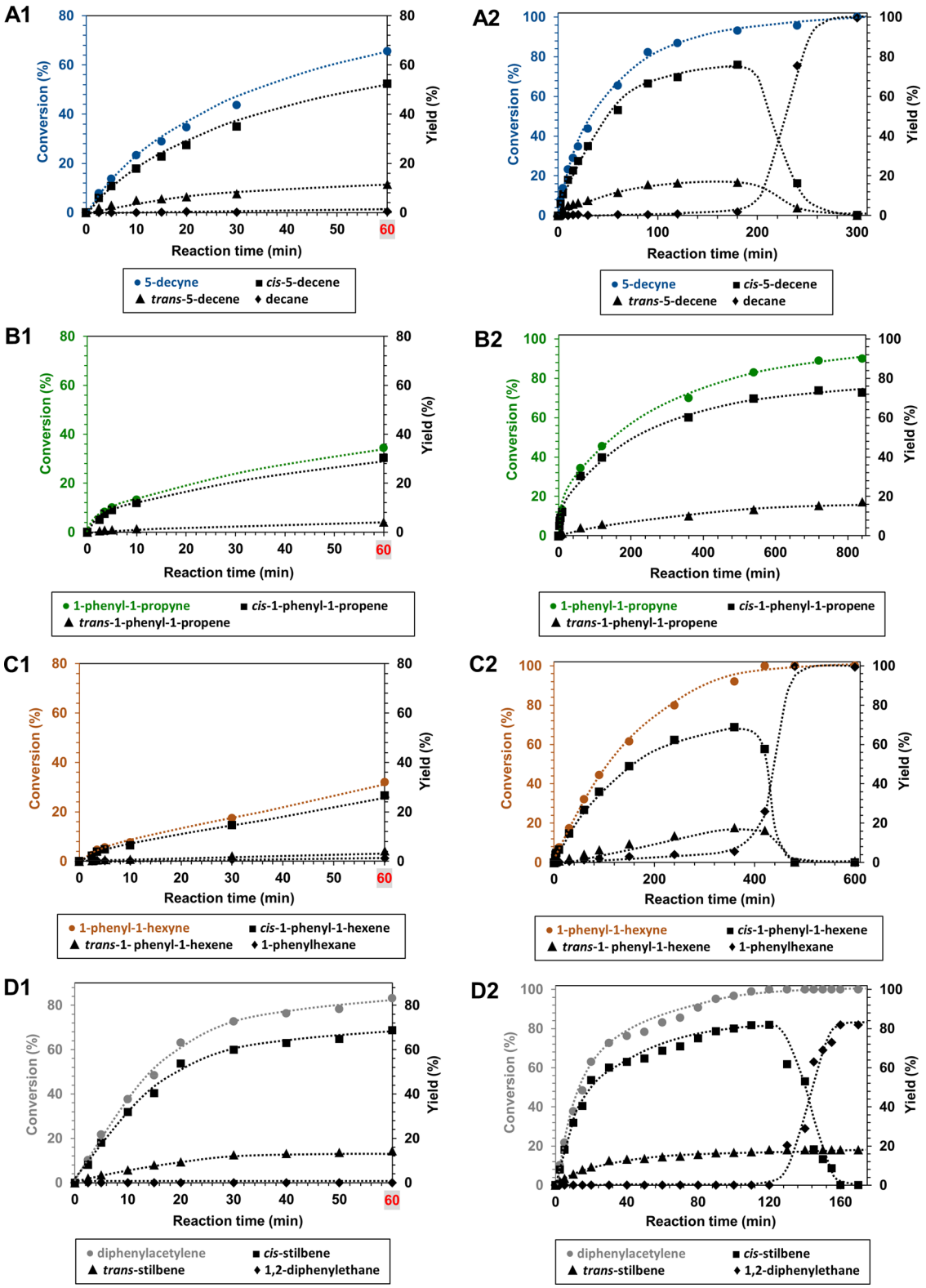

Figure 2. Reaction profiles of substrates **1**, **2**, **3**, and **4** on Pt/C with $(^{i}Pr)_2NEt$ as the hydrogen donor in the *p*-xylene solvent at 140 °C. Plots are shown for the first 1 h reaction time (A1, B1, C1, and D1) and for the full course of the reaction (A2, B2, C2, and D2). (All data points were taken from separate measurements, and no in situ sampling was applied. The dashed lines serve as a guide to the eyes.).

reaction rates were observed for substrates **1** and **4**, while the lowest value was determined for substrate **3** (Table 3). Pt was more active than Pd, comparing the normalized TOF values under the same reaction conditions in the presence of $(^{i}Pr)_2NEt$ as the H source. The TOF results obtained with Pt were two orders of magnitude higher than the ones measured with Pd (Table 3). Substrates **1**, **2**, and **3** had similar rates on Pd, while on Pt, the rate differences became more significant. On Pt, the reactivity trend followed the order **4** > **1** > **2** > **3** (Table 3 and Figure 3).

https://doi.org/10.1021/acscatal.0c05186
ACS Catal. 2021, 11, 5405−5415

Table 3. Initial Rates and TOF Values at 140 °C in *p*-Xylene as the Solvent of Substrates 1−4 on Pd/C− and Pt/C−(^{i}Pr)$_2$NEt Catalysts

	catalyst			
	Pd/C−(^{i}Pr)$_2$NEt		Pt/C−(^{i}Pr)$_2$NEt	
substrate	initial rate (mol g_{cat}^{-1} s^{-1})	TOF (s^{-1})[a]	initial rate (mol g_{cat}^{-1} s^{-1})	TOF (s^{-1})[a]
1	1.5×10^{-7}	7.4×10^{-4}	2.0×10^{-6}	1.8×10^{-2}
2	1.1×10^{-7}	7.0×10^{-4}	1.8×10^{-6}	1.2×10^{-2}
3	6.8×10^{-8}	4.4×10^{-4}	9.8×10^{-7}	6.5×10^{-3}
4	1.3×10^{-7}	7.2×10^{-4}	3.6×10^{-6}	3.2×10^{-2}

[a]Site density is based on H_2 chemisorption (see the Supporting Information). Reaction conditions: substrates **1**−**4** (1.0 mmol), alkyl amines (4.4 mmol), catalysts Pd/C (10 wt %, 0.1 mmol Pd) or Pt/C (10 wt %, 0.1 mmol Pt), *p*-xylene (1.5 mL), 140 °C, under Ar and atmospheric pressure. TOF values were determined from rates normalized to accessible metal sites and calculated in the unit of (mol $mol_{(surf.metal)}^{-1}$ s^{-1}) and shortened as (s^{-1}). For detailed kinetic measurements, see the Supporting Information part, Figures S2 and S3 and Tables S1−S8.

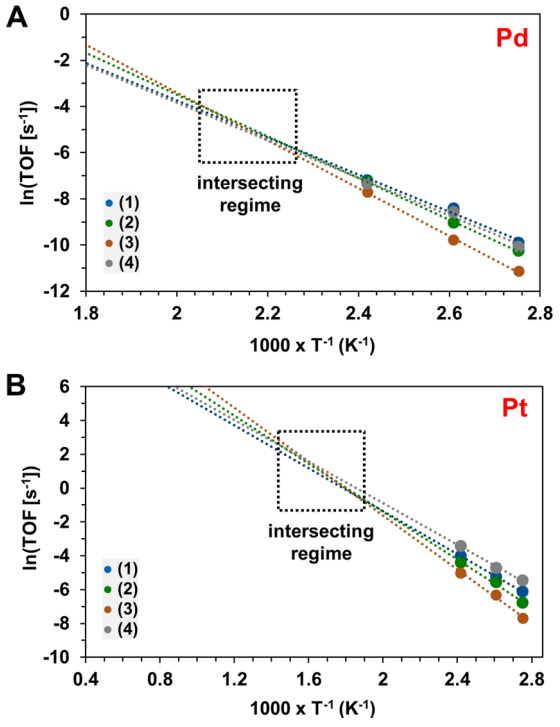

Figure 3. Arrhenius plots of Pd/C (A) and Pt/C (B) with (^{i}Pr)$_2$NEt as the H source with substrates **1**−**4** show an intersecting regime. The temperature range was 140−90 °C (see the Supporting Information).

We calculated the corresponding activation parameters (Table 4) for substrates **1**−**4** on Pd and Pt with (^{i}Pr)$_2$NEt as a reducing agent to obtain a better understanding of the selectivity and activity trends between the two noble metals. All of these parameters had higher values for Pd than for Pt, as originally expected from their different activation capacities. Activation energies determined on Pd were 14−20 kJ mol^{-1} higher than on Pt.

Three interesting phenomena were observed from the activation enthalpy and entropy changes (Table 4). One of them is the (highly) negative entropy values calculated for substrates **1**−**4** on both metals, which clearly indicate the presence of a strict transition state, the second is their linear correlation, and the third is the trend of their correlation (Figure 4).

In heterogeneous catalysis, the type of trend observed is called a "compensation effect" (Figure 4A,B),[8] namely, a linear correlation between the Arrhenius pre-exponential factor (A) and the experimentally determined activation energy (Figure 4B, Constable plot). The so-called isokinetic temperature (T_{iso}) (which may exist within or outside of experimentally accessible reaction conditions) can be extracted from the compensation plot;[8] this is an important parameter since all the considered reactions have the same rate constant at T_{iso} (Figure 4A,B). The first indication of the presence of a T_{iso} for the studied systems was the intersecting regime of the Arrhenius plots for both of the metals (Figure 3). In addition, correlating the $\Delta H^{\circ\ddagger}$ and $\Delta S^{\circ\ddagger}$ values calculated for the two metals again produced a beautiful linear relationship (Figure 4A), where the entropic gain is accompanied by increasing enthalpic values in the following increasing trend of the substrates: **1** ≤ **4** < **2** < **3** (Figure 4). Upon closely reviewing this trend, it can be seen that, surprisingly, the phenyl/phenyl (**4**)- and hexyl/hexyl (**1**)-substituted alkynes, the sterically most (**4**) and least (**1**) rigid derivatives, showed very similar activation parameters and a similarly high loss in terms of activation entropy (on both metals). The phenyl/methyl substituted alkyne (**2**) and phenyl/hexyl substituted alkyne (**3**) exhibited the largest enthalpy values, respectively (Table 4 and Figure 4A). This observation led us to conclude that the steric demand and rigidity of the substituents on the C≡C triple bond have a small effect on the activation parameters. However, the comparison of asymmetric substrates **2** and **3** shows that the higher flexibility of the hexyl group is realized in less negative activation entropies (Pd/C, −112 J mol^{-1} K^{-1}; Pt/C, −136 J mol^{-1} K^{-1}) (Table 4).

The isokinetic temperature is determined from the slope of the $\Delta H^{\circ\ddagger}$ vs $\Delta S^{\circ\ddagger}$ plot (Figure 4A) and from the correlation of ln(A) vs E_a (Figure 4B). Using the $\Delta H^{\circ\ddagger}$ vs $\Delta S^{\circ\ddagger}$ plot, T_{iso} values were 192.1 °C for Pd and 310.1 °C for Pt, while the Constable plots provided similar values of 190.3 °C (Pd) and 317.7 °C (Pt), indicating the close agreement of the two approaches. At the specified isokinetic temperatures, the specific adsorption properties, steric, and electronic behavior of the substrates support each other in the most appropriate way, leading to the highest rates under these reaction conditions (Figure 4A,B) (k_{iso} (Pd) = 7.1×10^{-3} (±0.1) s^{-1} (T_{iso} = 192.1 °C), k_{iso} (Pd) = 6.8×10^{-3} (±0.1) s^{-1} (T_{iso} = 190.3 °C); k_{iso} (Pt) = 2.2 (±0.2) s^{-1} (T_{iso} = 317.7 °C), k_{iso} (Pt) = 1.9 (±0.2) s^{-1} (T_{iso} = 310.1 °C)). Furthermore, based on the linear relationship of substrates **1**−**4** in the $\Delta H^{\circ\ddagger}$ vs $\Delta S^{\circ\ddagger}$ (and ln(A) vs E_a) plot (Figure 4), evidently, the mechanism leading to *cis* alkene dominance is the same for all substrates on the two metals.

Continuing the elucidation of the origin of *cis* alkene selectivity, the strongly negative entropy values indicate the presence of a highly ordered transition state on Pt and Pd surfaces, which points to the formation of a surface complex and to the presence of a concerted pathway involving the amine (Figure 5), rather than to a sequential route where the alkynes react with surface-adsorbed hydrogen.[4a] The specific adsorption properties of the alkynes likely play no determining role on the final outcome of the hydrogen transfer reaction since the reaction order is zero for substrates **1**−**4** on Pt/C (slightly negative for substrates **2** and **3**) (see the Supporting

https://doi.org/10.1021/acscatal.0c05186
ACS Catal. 2021, 11, 5405−5415

Table 4. Activation Parameters of Substrates 1−4

	catalyst					
	Pd/C−(^{i}Pr)$_2$NEt[a]			Pt/C−(^{i}Pr)$_2$NEt[a]		
substrate	E_a (kJ mol^{-1})	$\Delta H^{\circ\ddagger}$ (kJ mol^{-1})	$\Delta S^{\circ\ddagger}$ (J mol^{-1} K^{-1})	E_a (kJ mol^{-1})	$\Delta H^{\circ\ddagger}$ (kJ mol^{-1})	$\Delta S^{\circ\ddagger}$ (J mol^{-1} K^{-1})
1	67 (±8)	64 (±8)	−153 (±15)	53 (±2)	50 (±2)	−161 (±4)
2	75 (±2)	72 (±2)	−134 (±5)	59 (±6)	56 (±6)	−149 (±13)
3	86 (±3)	83 (±3)	−112 (±8)	66 (±6)	63 (±6)	−136 (±14)
4	68 (±8)	64 (±8)	−151 (±15)	51 (±4)	48 (±4)	−161 (±10)

[a]Reaction conditions: 140 °C/110 °C/90 °C, Pd/C (10 wt %, 0.1 mmol Pd), Pt/C (10 wt %, 0.1 mmol Pt), substrates **1**−**4** (1.0 mmol), alkyl amine (4.4 mmol), *p*-xylene (1.5 mL), under Ar and atmospheric pressure (for detailed kinetic dataset, see the Supporting Information, Tables S1−S8). Enthalpy and entropy values were calculated based on the Eyring equation (see the Supporting Information, Table S9). Error bars were calculated based on the LINEST method (linear least-squares method).

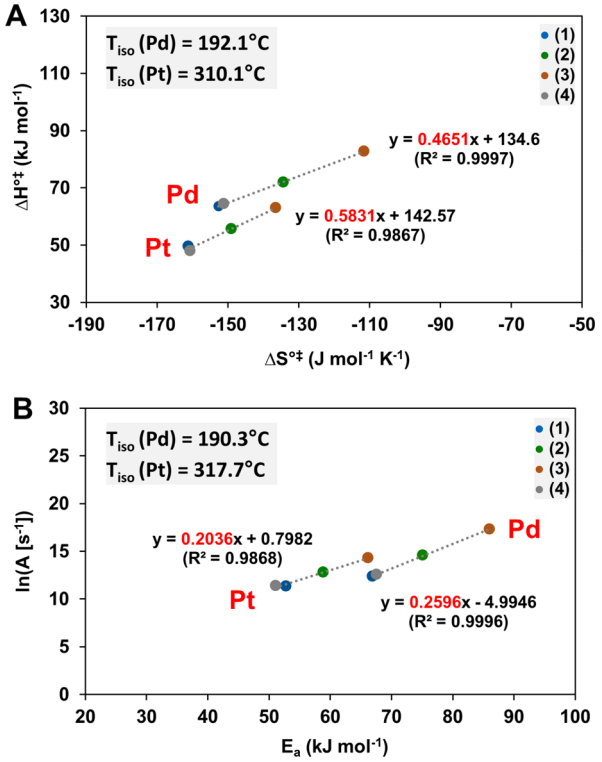

Figure 4. Compensation effect for substrates **1**−**4** on Pd/C and Pt/C in the presence of (^{i}Pr)$_2$NEt as the H source. $\Delta H^{\circ\ddagger}$ vs $\Delta S^{\circ\ddagger}$ correlation (A) and the Constable plot (B) for substrates **1**−**4** on Pd and Pt. T_{iso} values were calculated from the slope of the $\Delta H^{\circ\ddagger}$ vs $\Delta S^{\circ\ddagger}$ plot (A) and using $T_{iso} = (R \times \text{slope})^{-1} \times 1000$ (in K) from $\ln(A)$ vs E_a correlation (B). $\ln(A)$ values were calculated from the slope of the Arrhenius plots, and k_{iso} values were calculated from the equations: $\ln(A) = b \times E_a + c$; $b = (R \times T_{iso})^{-1}$ and $c = \ln(k_{iso})$.[8b]

Information, Figure S4 and Tables S10−S13). Additionally, the lack of over-hydrogenation on Pt/C with 1-EPyr as a H source points to the absence of pure metal hydride formation in favor of a more complex pathway (Figure 5, cycles I and II). We propose a reaction mechanism directly involving the amine based on the data set presented in the current study. In the first step of the reaction, insertion of the metal α to the C−H bond of the hydrogen donor molecule takes place followed by formation of a surface-linked metal hydride−alkylamine complex (Figure 5, cycle I). In the next steps, alkyne adduct formation and migratory insertion of H to form the corresponding alkene occur. For [M]/C−(R)$_3$N catalyst systems where over-reduction is hindered (i.e., Pd/C−(^{i}Pr)$_2$NEt, Pd/C−1-EPyr, Pt/C−1-EPyr)), the last step of the cycle involves desorption of the alkene as the final product (Figure 5).

In the case of over-hydrogenation, the intermediate alkene re-adsorbs, after the first hydrogen transfer, to serve as the starting material for the second cycle (Figure 5, cycle II).[4a,c] Within cycle II, as similarly proposed for the alkyne cycle, the intermediately forming metal hydride−alkylamine complex reacts with the alkene to form the alkene adduct (Figure 5, cycle II), followed by the migratory insertion of H to the C=C double bond that forms the alkane and enamine species. This enamine species was indirectly identified in our previous study of alkene hydrogenation based on the formation of unsaturated amines including pyridine and 1-ethyl-pyrrole.[4a] It is notable that the *cis* isomer dominates the alkene regime, independent of the alkyne substrate (Table 2). Even when over-hydrogenation takes place on Pt/C with (^{i}Pr)$_2$NEt, the intermediately formed alkene is the *cis* isomer (Table 2, entry 2A, substrates **1**, **3**, and **4**).

A high *cis*/*trans* isomer ratio is a relatively general observation for hydrogenation with molecular hydrogen on supported metals, which in most cases follows the Horiuti−Polanyi mechanism.[9] However, this selectivity has previously been attributed to high surface H-coverage,[10] which is not expected in our system due to the lack of over-hydrogenation and highly negative activation entropies. Thus, we were interested in whether the amines have an additional selectivity-determining role under the studied reaction conditions, rather than acting solely as a hydrogen source.

The zero reaction order of the starting alkynes (**1**−**4**), the compensated steric bulkiness, and the similar electronic properties of the substituents (phenyl and alkyl groups have weak electron donating ability) point to the tertiary alkyl amine playing a determining role on the selectivity and overall catalytic activity of the system. The sp hybridization of the carbon−carbon triple bond results in the perpendicular orientation of the σ-bond and two π-bonds (the bond angle of a sp-hybridized carbon is 180°).[5f] The close vicinity of the electrons in this geometric orientation creates molecules with less stability. The structure of the C≡C triple bond strongly influences the chemical reactivity of alkynes.[5a,f] Therefore, we assume that the stability, the chemical behavior of the intermediate metal hydride−alkylamine alkyne complex (alkyne adduct) (Figure 5), and the electronic effect on the alkene isomer play a decisive role in determining the overall selectivity. To explore this hypothesis, we performed experiments having diphenylacetylene (**4**) as the starting material on Pt/C with (^{i}Pr)$_2$NEt and we measured the selectivity dependence on the initial alkyne concentration (Figure 6).

https://doi.org/10.1021/acscatal.0c05186
ACS Catal. 2021, 11, 5405−5415

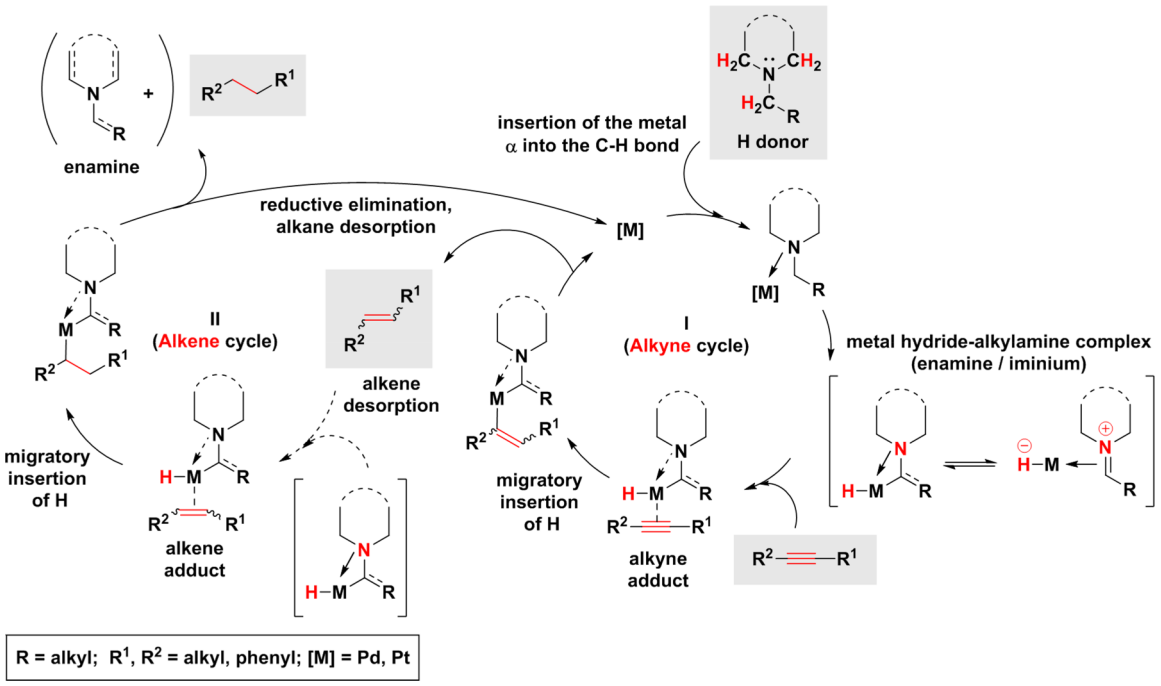

Figure 5. Schematic representation of the proposed mechanism of hydrogen transfer reaction of alkynes to alkenes (I) and alkenes to C−C single-bonded compounds (II) on carbon-supported Pd and Pt catalysts with tertiary alkyl amines as hydrogen donor molecules.

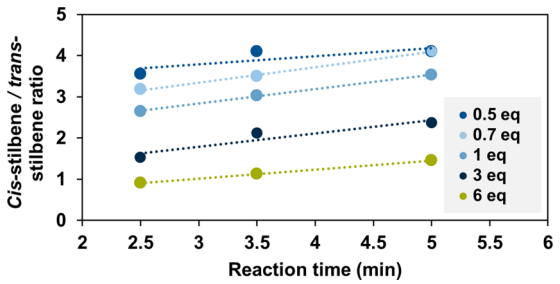

Figure 6. *Cis*-stilbene/*trans*-stilbene isomer ratio changes with increasing initial alkyne concentration (0.5−6 equiv of **4** to 4.4 equiv of $(^{i}Pr)_2NEt$ amine as the hydrogen donor on Pt/C). (The dashed lines serve as a guide to the eyes.).

As mentioned above, the reaction order of **4** on Pt/C−$(^{i}Pr)_2NEt$ catalytic system is zero (see the Supporting Information, Figure S4 and Table S13). However, an increased concentration of the starting alkyne, relative to the amine, hinders formation of the *cis* isomer (Figure 6). Conversely, higher equivalents (equiv) of the amine relative to substrate **4** favor formation of the *cis* isomer. Determination of the reaction order for amines shows a modest fractional dependence in the regime of 1−5.2 equiv ($(^{i}Pr)_2NEt$, 0.27; 1-EPyr, 0.15) of the amines, which were considered to be zero (see the Supporting Information, Figure S5 and Tables S14 and S15). This observation and the fact that the H donor species was always used in an excess amount (substrate/amine ratio is 1/4.4) suggest that any possible dependency with amine concentration should take place at a substrate/amine ratio higher than 1/1.

Cross-experiments demonstrate that no reaction takes place in the absence of the amine. Parallel experiments with homogeneous catalysts ($Rh(PPh_3)_3Cl$), $Pd(OAc)_2$ + 2 equiv of PPh_3, $Pd(PPh_3)_4$) were carried out in the presence of the amines ($(^{i}Pr)_2NEt$, 1-EPyr) under the same reaction conditions as with Pd/C and Pt/C. Only the Wilkinson's complex was active, which showed minor conversion only for substrate **4** ($(^{i}Pr)_2NEt$, 2%; 1-EPyr, 1%), while the Pd-based molecular catalysts showed no activity with the entire substrate scope. Atomic absorption spectroscopy (AAS) shows a negligible amount of Pd (<0.005 mg L^{-1}) and Pt (<0.001 mg L^{-1}) in the liquid phase after reaction completion. Additionally, poisoning experiments with 1,10-phenanthroline (phen) showed an insignificant change in the conversion of substrate **4** on Pt/C with $(^{i}Pr)_2NEt$ at 140 °C in the *p*-xylene solvent, which demonstrates the heterogeneous nature of the reaction (reference experiment: 48% conversion after 15 min (Figure 2D1,D2); poisoning experiments: with 0.1 and 0.5 equiv of phen relative to the amount of Pt active sites under the same reaction conditions both showed 46% conversion after 15 min).

Due to the spectroscopic challenges in measuring the intermediately forming surface complexes, we performed DFT calculations to elucidate the molecular origin of the observed selectivity and the sequential hydrogenation mechanism using the Vienna ab initio simulation program (VASP) 5.4.[11] The noble metal surfaces were modeled using four-layer slabs of Pt(111) and Pd(111). The bottom two layers of the slabs were constrained to maintain the bulk metal structure. All calculations used the projector-augmented wave (PAW) method[12] with the Perdew−Burke−Ernzerhof (PBE) exchange correlation functional[13] and Grimme's D3 dispersion correction with Becke−Jonson damping.[14] Slab calculations used a 3 × 3 × 1 Monkhorst−Pack *k*-point grid to sample the Brillouin zone (see the Supporting Information for additional details).

The sequential nature of the hydrogenation process suggests the alkyne reactants and alkene products must have different binding energies. Therefore, we computed the binding energies of two different alkynes and their corresponding alkene products: 2-butyne, the simplest possible model alkyne that can yield *cis* and *trans* products (note that 2-butyne served as a

https://doi.org/10.1021/acscatal.0c05186
ACS Catal. 2021, 11, 5405−5415

model alkyne substrate only for theoretical studies) and substrate **2** (1-phenyl-1-propyne) (Figures 1 and 2). On both Pt(111) and Pd(111), the alkynes bind at fcc (face-centered-cubic) sites, with stronger binding energies than the corresponding alkenes that bind across two metal atoms in a di-σ fashion (Table 5, corresponding geometries in Figures S6 and S7). The difference in binding affinities is particularly notable when comparing 2-butyne to 2-butene, where there are no significant interactions between the substituents and surface. The stronger binding of the triple-bonded alkyne allows it to displace the alkene before it becomes further hydrogenated, resulting in the sequential hydrogenation observed experimentally on Pt/C (Figure 3). Once the alkyne has been converted to an alkene, over-hydrogenation to the alkane can occur in some cases, as shown in Figure 3A2,C2,D2. For substrate **2**, which does not experience sequential over-hydrogenation, the binding energy of the alkyne is comparable to those of the *cis* and *trans* alkenes due to the strong interaction between the phenyl group of the alkenes and the metal surface (whereas there is no such interaction in the 2-butyne case). This can be related to the lack of over-hydrogenation since the alkene is especially stable on the surface, which may inhibit further saturation (Table 5). It is notable that all components with a phenyl group bind more strongly on Pd, while the others bind more strongly to Pt.

Table 5. Binding Energies of Alkynes, Alkenes, and Amines on Pd(111) and Pt(111) Surfaces

	binding energy (eV)	
adsorbate	Pd(111)	Pt(111)
2-butyne	−2.468	−2.780
cis-2-butene	−1.521	−1.722
trans-2-butene	−1.478	−1.722
1-phenyl-1-propyne (**2**)	−3.507	−3.174
cis-1-phenyl-1-propene	−3.244	−3.030
trans-1-phenyl-1-propene	−3.285	−3.075
1-EPyr	−1.704	−1.800
$(^{i}Pr)_2NEt$	−1.506	−1.595

DFT calculations were able to determine the cause of the observed selectivity trend, providing mechanistic insights into the role of the amine. For calculations of the reaction energetics, 1-EPyr was chosen as the hydrogen donor (due to its structural simplicity in comparison with $(^{i}Pr)_2NEt$) and Pt(111) as the metal surface. Calculations with substrate **2** could be directly compared to the experimental results (Table 2, entry 2B), while those for 2-butyne provided further general insights.

The experimental results indicated that the amine controls the reaction selectivity. In fact, calculations with bare metal surfaces show no evidence of the *cis* selectivity observed in the presence of the amine (Table 6). Analogously, previous studies of selectivity for direct hydrogenation of *cis*- and *trans*-2-butene[10b] have shown that significant coverage of the metal surface by hydrogen (>0.44 mL) is required to obtain *cis* isomer favorability. In our transfer hydrogenation reactions, however, there is no hydrogen coverage of the surface, and clearly, the metal surface alone does not confer *cis* selectivity. So, we conclude that the amine induces *cis* selectivity upon sufficient coverage of the surface, analogous to the effect of hydrogen on the surface in direct hydrogenation reactions. For comparison, we note that our calculations in the gas phase show the *trans* isomers of both 2-butene and 1-phenyl-1-propene are energetically favored. The Pt surface had a negligible effect on the relative energetics of the 2-butene isomers (binding energies within 10^{-3} eV) and actually disfavored the *cis*-1-phenyl-1-propene isomer in comparison to the gas phase. On the other hand, the Pd surface brought the 2-butene isomers to approximately equal energy but similarly disfavored the *cis*-1-phenyl-1-propene isomer. Taken together, there is no indication that the *cis* isomer would be favored on either surface in the isolated case; in the case of substrate **2**, interactions with the surfaces actually further disfavor the *cis* isomer (in contrast with the experimental data).

Table 6. *Cis*−*Trans* Isomerization Energies of Alkenes in the Gas Phase and on Pt(111) and Pd(111) Surfaces

	$E_{cis}-E_{trans}$ (kJ mol^{-1})		
alkene	gas	Pd(111)	Pt(111)
2-butene	+3.8	−0.3	+3.9
1-phenyl-1-propene	+8.7	+12.6	+13.1

From the experimental selectivity results, we hypothesized that a metal hydride−alkylamine alkyne complex (alkyne adduct, Figure 5) could be a crucial reaction intermediate. The increased surface coverage by the amine correlates with increased selectivity, decreasing drastically when the relative concentration of the alkyne is increased (Figure 6). The increased concentration of amine produces isolated reaction sites where alkynes can bind; interactions between the amine and alkyne at these sites might produce *cis* selectivity. Therefore, we investigate the molecular origin of this effect by computing the reaction energetics for the hydrogenation of **2** by 1-EPyr on Pt(111). Analogously to the Horiuti−Polanyi mechanism known for hydrogenation with molecular H_2,[9] hydrogen atoms are added sequentially to the alkyne. However, in our case, the hydrogen is being transferred from a metal hydride−alkylamine complex (Figure 5) rather than from a hydrogen-covered surface. First, a hydrogen atom is added to one of the carbons, while the other remains more closely bound to the surface. The energetics of this first hydrogenation step cannot confer any selectivity as it is identical for both products (Figure S8). Next, a second hydrogen is transferred to the mono-hydrogenated intermediate to produce an alkene product (Figure 7), which can desorb and be replaced by another alkyne. This second hydrogenation step (Figure 7C) can confer product selectivity as the monohydrogenated intermediate will interact differently with the amine depending on its orientation. Additionally, the interactions between the intermediate and amine will depend on the amount of surface coverage. To simulate the effect of surface coverage, calculations were performed on periodic unit cells of two different sizes ($a \times b$ = 4 × 4 and 4 × 5). The smaller unit cell allowed for closer packing of the adsorbates (see the Supporting Information, Figure S9), producing a higher effective coverage. The second hydrogenation step that determines the overall selectivity was computed at both coverage levels (Figure 7).

The second hydrogenation process can be broken down into two steps: (a) H transfer from 1-EPyr to the Pt surface to form a partially saturated metal hydride-alkylamine yne/ene intermediate (**I** → **II**) (yne/ene refers to the semisaturation state of the alkyne) and (b) transfer of H from Pt to the yne/ene intermediate to produce the alkene (*cis*-**III**/*trans*-**III**,

https://doi.org/10.1021/acscatal.0c05186
ACS Catal. 2021, 11, 5405−5415

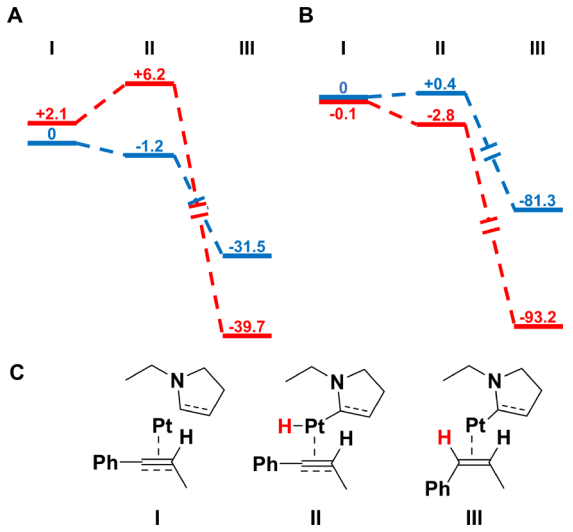

Figure 7. Comparison of reaction energetics (in kJ mol^{-1}) at high (A) and low (B) coverage for the second saturation step of transfer hydrogenation of **2** by 1-EPyr on Pt. Energetics for forming the *cis* conformer are shown in blue and energetics for the *trans* conformer are shown in red. (C) Schematic representation of intermediates **I**, **II**, and **III** for the formation of the *cis* isomer.

Figure 7C). The energetics of the two steps at high and low coverage are shown in Figure 7, while the structures of the key metal hydride−alkylamine yne/ene intermediates are shown in Figure 8 (all 12 intermediates are shown in Figure S10).

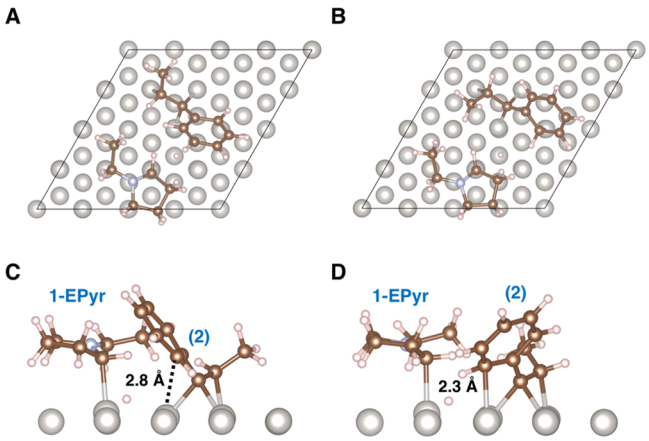

Figure 8. Top (A, B) and side (C, D) views of (monohydrogenated) *cis* and *trans* yne/ene-Pt alkylamine intermediates, respectively, at high surface coverage (i.e., species **II** in Figure 7A). The amine (1-EPyr) and monohydrogenated alkyne (**2**) are labeled. The distance between the nearest phenyl C atom and a surface Pt atom is indicated.

The energetics of the selectivity determining hydrogenation step were computed at two amine coverage levels (high coverage, Figure 7A; low coverage, Figure 7B). Interestingly, the (monohydrogenated) *trans* yne/ene metal hydride−alkylamine complex (*trans*-**II**, Figure 7C) (favored by 3.2 kJ mol^{-1}) and the corresponding *trans* product are more stable than the *cis* isomer at low coverage. However, at higher coverage, compound *cis*-**II** (Figure 7C) is more stable, resulting in the measured *cis* selectivity. This high coverage case is more relevant to the experimental conditions, where 1-EPyr was used in excess. In both cases, the *cis*-**II**/*trans*-**II** complex is the highest energy intermediate, allowing for selectivity control (Figure 8). At high coverage, intermediate *cis*-**II** (Figure 7C) is favored by 7.4 kJ mol^{-1}, implying a roughly 9/1 Boltzmann population ratio at 140 °C. These results are in excellent agreement with the experimental findings, where a *cis*/*trans* ratio of 31/3 (yield (%)) was measured (Table 2, entry 2B). It is important to note that the selectivity trend arises from the relative stabilities of the corresponding metal hydride−alkylamine surface complexes (*cis*-**II** and *trans*-**II**), rather than the *cis* and *trans* products. The *trans* product remains energetically favorable at high coverage by 8.2 kJ/mol (*trans*-**II**, Figure 7C), but the instability of the corresponding surface complex intermediate impairs its formation. Formation of the alkene product is always highly favorable from the partially hydrogenated metal hydride−alkylamine intermediate (*cis*-**II**/*trans*-**II**), so the differences in product stability have little relevance to the reaction selectivity.

As shown in Figure 8A,B, the monohydrogenated **2** intermediate binds at an fcc site, with the hydrogenated end on top of a Pt atom and the other end at a bridge site between two Pt atoms. The phenyl group adopts the orientation that maximizes the interaction between the *p* orbital of one of its carbon atoms and a Pt atom. After donating an H atom from the amine to Pt, the intermediate forms a C−Pt bond of ∼2.3 Å length (*trans*-**II**, Figure 8D). Interactions between this strongly bound species and the monohydrogenated **2** result in stereoselectivity. Alternative orientations for these intermediates were considered (representative examples are provided in the Supporting Information, Figures S11 and S12).

The reaction energetics computed for 2-butyne in the presence of 1-EPyr shows the same trend although with a somewhat smaller effect on selectivity (see the Supporting Information, Figures S13 and S14). These results suggest the generality of the selectivity trend across alkynes. Also, these calculations suggest that at least one larger functional group may be required to obtain reaction selectivity comparable to those measured for substrates **1**−**4**.

Further analysis of the substrate **2** system was performed to analyze the molecular origin of the stabilization of the partially saturated *cis* yne/ene Pt hydride−alkylamine complex at high coverage (*cis*-**II**, Figure 7A). The amine has two distinct effects on the relative stabilities of the monohydrogenated alkyne intermediates: a structural effect arising from geometric distortions to the alkyne and an electronic effect originating from interactions between the amine and the alkyne. Both of these factors could account for the stabilization of the *cis* isomer.

The effect of structural distortions was computed at high and low surface coverage (see the Supporting Information). We find the energy change due to distortions is larger for the *cis* isomer at both high and low surface coverage (see the Supporting Information, Table S16). As shown in Figure 8, the amine prevents the phenyl group of the *cis* isomer (a C−Pt distance of 2.8 Å) (*cis*-**II**, Figure 8C) from interacting closely with the surface, while the *trans* isomer (a C−Pt distance of 2.3 Å) (*trans*-**II**, Figure 8D) does not exhibit an analogous steric impediment. Therefore, the steric hindrance always destabilizes the *cis* isomer relative to the *trans* isomer. This implies that the electronic effect of the amine must be responsible for the *cis* stabilization at high coverage. The electronic effect of the amine stabilizes the *cis* isomer by 11.1 and 8.3 kJ mol^{-1} at high and low coverage, respectively (Table S17). This favorable electronic effect arises from the closer interaction between the phenyl group of the *cis* monohydrogenated intermediate and

https://doi.org/10.1021/acscatal.0c05186
ACS Catal. 2021, 11, 5405−5415

the amine (Figure 8C). The electronic effect is dominant at high coverage, where the structural distortions are similar for the two isomers. While the structural distortions always favor the *trans* isomer, higher coverage makes the effect of structural distortions larger in the *trans* case (from +21.3 to +27.0 kJ mol^{-1}) and slightly smaller in the *cis* case (from +30.6 to +29.9 kJ mol^{-1}). The 9.1 kJ mol^{-1} shift in the relative magnitudes of the structural distortions is the major component of the total 10.6 kJ mol^{-1} shift toward the *cis* isomer at high coverage. At high coverage, the two isomers experience comparable steric effects from the amine, leading to the dominance of the electronic stabilization of the *cis* isomer.

Overall, the electronic effect always stabilizes the *cis* isomer and becomes more stabilizing at high coverage. On the other hand, the structural effect always destabilizes the *cis* isomer but becomes less destabilizing at high coverage. The interplay of these two effects on the metal hydride−alkylamine complexes ultimately stabilizes the *cis* isomer at high amine concentrations consistent with the experiment.

3. CONCLUSIONS

We have investigated the selective transfer hydrogenation of substituted alkynes with tertiary alkyl amines as H donors on noble metals. The combined experimental and theoretical analysis supports a sequential mechanism in which the *cis* alkene is initially formed, sometimes followed by further hydrogenation to the C−C single-bonded derivatives when using the Pt/C−$(^{i}Pr)_2$NEt catalyst system.

We have shown high activity with partial to complete conversion at 140 °C in the *p*-xylene solvent. Observation of the compensation effect allowed us to determine the corresponding isokinetic temperatures for which the highest rate constant is obtained. Our theoretical analysis has identified the critical role of the tertiary alkyl amines. The presence of the H donor molecule induces steric and electronic effects on the metal hydride−alkylamine alkyne intermediate (alkyne adduct), resulting in selectivity toward the *cis* isomer. Our combined experimental and computational analysis shows that significant surface coverage with a tertiary amine can induce selective conversion of alkynes into *cis* alkene isomers.

■ ASSOCIATED CONTENT

Supporting Information

The Supporting Information is available free of charge at https://pubs.acs.org/doi/10.1021/acscatal.0c05186.

DFT coordinates of TH of alkynes (ZIP)

Experimental procedures and materials, mode of calculations, representative GC spectra, kinetic measurements and determination of activation parameters, determination of activation enthalpy ($\Delta H^{\circ\ddagger}$) and activation entropy ($\Delta S^{\circ\ddagger}$), reaction order determination of substrates **1**−**4**, reaction order determination of $(^{i}Pr)_2$NEt and 1-EPyr in the presence of substrate **4**, and computational details (PDF)

■ AUTHOR INFORMATION

Corresponding Author

Eszter Baráth − *Department of Chemistry and Catalysis Research Center, Technische Universität München, Garching D-85748, Germany;* orcid.org/0000-0001-8494-3388; Email: eszter.barath@tum.de

Authors

Gabriel J. Roeder − *Department of Chemistry and Catalysis Research Center, Technische Universität München, Garching D-85748, Germany*

H. Ray Kelly − *Department of Chemistry, Yale University, New Haven, Connecticut 06520, United States;* orcid.org/0000-0003-3811-0662

Guoju Yang − *Department of Chemistry and Catalysis Research Center, Technische Universität München, Garching D-85748, Germany*

Thomas J. Bauer − *Department of Chemistry and Catalysis Research Center, Technische Universität München, Garching D-85748, Germany*

Gary L. Haller − *Department of Chemistry and Catalysis Research Center, Technische Universität München, Garching D-85748, Germany; Department of Chemical and Environmental Engineering, Yale University, New Haven, Connecticut 06520, United States;* orcid.org/0000-0001-8482-5488

Victor S. Batista − *Department of Chemistry, Yale University, New Haven, Connecticut 06520, United States;* orcid.org/0000-0002-3262-1237

Complete contact information is available at: https://pubs.acs.org/10.1021/acscatal.0c05186

Author Contributions

#G.J.R. and H.R.K. contributed equally. The manuscript was written through contributions of all authors. All authors have given approval to the final version of the manuscript.

Funding

V.S.B. acknowledges support by the Air Force Office of Scientific Research (AFOSR) grant #FA9550-13-1-0020.

Notes

The authors declare no competing financial interest.

■ ACKNOWLEDGMENTS

E.B. thanks J. A. Lercher for providing the necessary facilities in order to carry out the experiments and to H. Shi for extensive discussions. V.S.B. acknowledges allocations of high-performance computer time from the National Energy Research Scientific Computing Center (NERSC), Department of Defense High Performance Computing Modernization Program (DOD HPCMP), and the Yale Center for Research Computing. G.Y. acknowledges the China Scholarship Council (CSC) and the 111 Project (B17020) of China for their financial support.

■ REFERENCES

(1) (a) Meemken, F.; Baiker, A. Recent Progress in Heterogeneous Asymmetric Hydrogenation of C=O and C=C Bonds on Supported Noble Metal Catalysts. *Chem. Rev.* **2017**, *117*, 11522−11569. (b) Baráth, E. Hydrogen Transfer Reactions of Carbonyls, Alkynes, and Alkenes with Noble Metals in the Presence of Alcohols/Ethers and Amines as Hydrogen Donors. *Catalysts* **2018**, *8*, 671−695. (c) Wang, D.; Astruc, D. The Golden Age of Transfer Hydrogenation. *Chem. Rev.* **2015**, *115*, 6621−6686. (d) Slack, E. D.; Gabriel, C. M.; Lipshutz, B. H. A Palladium Nanoparticle−Nanomicelle Combination for the Stereoselective Semihydrogenation of Alkynes in Water at Room Temperature. *Angew. Chem., Int. Ed.* **2014**, *53*, 14051−14054. (e) Liang, S.; Hammond, G. B.; Xu, B. Supported gold nanoparticles catalyzed *cis*-selective semihydrogenation of alkynes using ammonium formate as the reductant. *Chem. Commun.* **2016**, *52*, 6013−6016. (f) Zhong, J.-J.; Liu, Q.; Wu, C.-J.; Meng, Q.-Y.; Gao, X.-W.; Li, Z.-J.;

Chen, B.; Tung, C.-H.; Wu, L.-Z. Combining visible light catalysis and transfer hydrogenation for *in situ* efficient and selective semi-hydrogenation of alkynes under ambient conditions. *Chem. Commun.* **2016**, *52*, 1800−1803.

(2) Gierz, V.; Urbanaite, A.; Seybolt, A.; Kunz, D. Rhodium Complexes Bearing 1,10-Phenanthroline Analogue Bis-NHC Ligands Are Active Catalysts for Transfer Hydrogenation of Ketones. *Organometallics* **2012**, *31*, 7532−7538.

(3) (a) Klomp, D.; Hanefeld, U.; Peters, J. A. Transfer hydrogenation including the Meerwein-Ponndorf-Verley reduction. In *The Handbook of Homogeneous Hydrogenation*; de Vries, J.G.; Elsevier, C.J. Eds.; WILEY-VCH Verlag GmbH & Co. KGaA, 2007; Chapter 20, pp. 585−630. (b) Hynes, J. T.; Klinman, J. P.; Limbach, H.-H.; Schowen, R. L. Eds. Hydrogen transfer in organic and organometallic reactions. *In Hydrogen-Transfer Reactions*; WILEY-VCH Verlag GmbH & Co. KGaA, 2007; Part V, Chapter 18−21, pp. 563−634.

(4) (a) Yang, G.; Bauer, T. J.; Haller, G. L.; Baráth, E. H-Transfer reactions of internal alkenes with tertiary amines as H-donors on carbon supported noble metals. *Org. Biomol. Chem.* **2018**, *16*, 1172−1177. (b) Muzart, J. On the behavior of amines in the presence of Pd^0 and Pd^{II} species. *J. Mol. Catal. A: Chem.* **2009**, *308*, 15−24. (c) Coquerel, Y.; Brémond, P.; Rodriguez, J. Pd−H from Pd/C and triethylamine: Implications in palladium catalysed reactions involving amines. *J. Organomet. Chem.* **2007**, *692*, 4805−4808. (d) Zhang, X.; Fried, A.; Knapp, S.; Goldman, A. S. Novel synthesis of enamines by iridium-catalyzed dehydrogenation of tertiary amines. *Chem. Commun.* **2003**, 2060−2061. (e) Lu, Y. J.; Zhang, X.; Malakar, S.; Krogh-Jespersen, K.; Hasanayn, F.; Goldman, A. S. Formation of Enamines via Catalytic Dehydrogenation by Pincer-Iridium Complexes. *J. Org. Chem.* **2020**, *85*, 3020−3028. (f) Yoshimura, N.; Moritani, I.; Shimamura, T.; Murahashi, S. Synthesis of unsymmetrical secondary and tertiary amines from amines by palladium catalyst. *J. Am. Chem. Soc.* **1973**, *95*, 3038−3039. (g) Mukherjee, S.; Yang, J. W.; Hoffmann, S.; List, B. Asymmetric Enamine Catalysis. *Chem. Rev.* **2007**, *107*, 5471−5569. (h) Erkkilä, A.; Majander, I.; Pihko, P. M. Iminium Catalysis. *Chem. Rev.* **2007**, *107*, 5416−5470. (i) Murahashi, S.; Hirano, T.; Yano, T. Palladium Catalyzed Amine Exchange Reaction of Tertiary Amines. Insertion of Palladium(0) into Carbon-Hydrogen Bonds. *J. Am. Chem. Soc.* **1978**, *100*, 348−350.

(5) (a) Delgado, J. A.; Benkirane, O.; Claver, C.; Curulla-Ferré, D.; Godard, C. Advances in the preparation of highly selective nanocatalysts for the semi-hydrogenation of alkynes using colloidal approaches. *Dalton Trans.* **2017**, *46*, 12381−12403. (b) Gigola, C. E.; Aduriz, H. R.; Bodnariuk, P. Particle size effect in the hydrogenation of acetylene under industrial conditions. *Appl. Catal.* **1986**, *27*, 133−144. (c) Chinchilla, R.; Nájera, C. Chemicals from Alkynes with Palladium Catalysts. *Chem. Rev.* **2014**, *114*, 1783−1826. (d) Domínguez-Domínguez, S.; Berenguer-Murcia, Á.; Pradhan, B. K.; Linares-Solano, Á.; Cazorla-Amorós, D. Semihydrogenation of Phenylacetylene Catalyzed by Palladium Nanoparticles Supported on Carbon Materials. *J. Phys. Chem. C* **2008**, *112*, 3827−3834. (e) Garcia, P. E.; Lynch, A. S.; Monaghan, A.; Jackson, S. D. Using modifiers to specify stereochemistry and enhance selectivity and activity in palladium-catalysed, liquid phase hydrogenation of alkynes. *Catal. Today* **2011**, *164*, 548−551. (f) Clayden, J.; Greeves, N.; Warren, S. Structure of molecules. In *Organic Chemistry*; OXFORD University Press: Oxford, UK, 2012; Chapter 4, pp. 80−106.

(6) (a) Lindlar, H. Ein neuer Katalysator für selektive Hydrierungen. *Helv. Chim. Acta* **1952**, *35*, 446−450. (b) Lindlar, H.; Dubuis, R. Palladium Catalyst for Partial Reduction of Acetylenes. *Org. Synth.* **2003**, *46*, 89. (c) Vilé, G.; Almora-Barrios, N.; Mitchell, S.; López, N.; Pérez-Ramírez, J. From the Lindlar Catalyst to Supported Ligand-Modified Palladium Nanoparticles: Selectivity Patterns and Accessibility Constraints in the Continuous-Flow Three-Phase Hydrogenation of Acetylenic Compounds. *Chem. - Eur. J.* **2014**, *20*, 5926−5937. (d) García-Mota, M.; Gómez-Díaz, J.; Novell-Leruth, G.; Vargas-Fuentes, C.; Bellarosa, L.; Bridier, B.; Pérez-Ramírez, J.; López, N. A density functional theory study of the 'mythic' Lindlar hydrogenation catalyst. *Theor. Chem. Acc.* **2011**, *128*, 663−673.

(7) (a) Brown, C. A. The hydrogenation of hex-1-yne over borohydride-reduced catalysts. Evidence concerning the mechanism of reduction. *J. Chem. Soc. D* **1970**, 139−140. (b) Brus, L. E. Electron−electron and electron-hole interactions in small semiconductor crystallites: The size dependence of the lowest excited electronic state. *J. Chem. Phys.* **1984**, *80*, 4403. (c) Bamberger, E. Ueber das Phenylhydroxylamin. *Ber. Dtsch. Chem. Ges.* **1894**, *27*, 1548−1557. (d) West, P. R.; Davis, G. C. The Synthesis of Diarylnitrones. *J. Org. Chem.* **1989**, *54*, 5176−5180. (e) López, N.; Vargas-Fuentes, C. Promoters in the hydrogenation of alkynes in mixtures: Insights from density functional theory. *Chem. Commun.* **2012**, *48*, 1379−1391.

(8) (a) Bond, G. C.; Keane, M. A.; Kral, H.; Lercher, J. A. Compensation Phenomena in Heterogeneous Catalysis: General Principles and a Possible Explanation. *Catal. Rev.* **2000**, *42*, 323−383. (b) Bratlie, K. M.; Li, Y.; Larsson, R.; Somorjai, G. A. Compensation Effect of Benzene Hydrogenation on Pt(111) and Pt(100) Analyzed by the Selective Energy Transfer Model. *Catal. Lett.* **2008**, *121*, 173−178. (c) Keane, M. A.; Larsson, R. Isokinetic behavior in the gas phase hydrogenation of nitroarenes over Au/TiO_2: Application of the selective energy transfer model. *React. Kinet., Mech. Catal.* **2012**, *106*, 267−288. (d) Larsson, R. On the compensation effect and selective oxidation reactions. *Catal. Today* **1987**, *1*, 93−99. (e) Bligaard, T.; Honkala, K.; Logadottir, A.; Nørskov, J. K.; Dahl, S.; Jacobsen, C. J. H. On the Compensation Effect in Heterogeneous Catalysis. *J. Phys. Chem. B* **2003**, *107*, 9325−9331.

(9) Horiuti, I.; Polanyi, M. Exchange reactions of hydrogen on metallic catalysts. *Trans. Faraday Soc.* **1934**, *30*, 1164−1172.

(10) (a) Li, J.; Fleurat-Lessard, P.; Zaera, F.; Delbecq, F. Mechanistic investigation of the *cis/trans* isomerization of 2-butene on Pt(1 1 1): DFT study of the influence of the hydrogen coverage. *J. Catal.* **2014**, *311*, 190−198. (b) Li, J.; Fleurat-Lessard, P.; Zaera, F.; Delbecq, F. Switch in Relative Stability between *cis* and *trans* 2-Butene on Pt(111) as a Function of Experimental Conditions: A Density Functional Theory Study. *ACS Catal.* **2018**, *8*, 3067−3075.

(11) (a) Kresse, G.; Hafner, J. *Ab initio* molecular dynamics for liquid metals. *Phys. Rev. B* **1993**, *47*, 558−561. (b) Kresse, G.; Hafner, J. *Ab initio* molecular-dynamics simulation of the liquid-metal−amorphous-semiconductor transition in germanium. *Phys. Rev. B* **1994**, *49*, 14251−14269. (c) Kresse, G.; Furthmüller, J. Efficiency of *ab-initio* total energy calculations for metals and semiconductors using a plane-wave basis set. *Comput. Mater. Sci.* **1996**, *6*, 15−50. (d) Kresse, G.; Furthmüller, J. Efficient iterative schemes for *ab initio* total-energy calculations using a plane-wave basis set. *Phys. Rev. B* **1996**, *54*, 11169−11186.

(12) (a) Blöchl, P. E. Projector augmented-wave method. *Phys. Rev. B* **1994**, *50*, 17953−17979. (b) Kresse, G.; Joubert, D. From ultrasoft pseudopotentials to the projector augmented-wave method. *Phys. Rev. B* **1999**, *59*, 1758−1775.

(13) Perdew, J. P.; Burke, K.; Ernzerhof, M. Generalized Gradient Approximation Made Simple. *Phys. Rev. Lett.* **1996**, *77*, 3865−3868.

(14) (a) Grimme, S.; Antony, J.; Ehrlich, S.; Krieg, H. A consistent and accurate *ab initio* parametrization of density functional dispersion correction (DFT-D) for the 94 elements H-Pu. *J. Chem. Phys.* **2010**, *132*, 154104. (b) Grimme, S.; Ehrlich, S.; Goerigk, L. Effect of the Damping Function in Dispersion Corrected Density Functional Theory. *J. Comput. Chem.* **2011**, *32*, 1456−1465.

https://doi.org/10.1021/acscatal.0c05186
ACS Catal. 2021, 11, 5405−5415